

Optimization and dimensioning of stand-alone systems: enhancing MPPT efficiency through DLGA integration

Moufida Saadi, Dib Djalel, Kadir Erkan

Electrical and Engineering Laboratory (LABGET), Faculty of Electrical Engineering, University of Tebessa, Tebessa, Algeria

Article Info

Article history:

Received May 5, 2023

Revised Nov 4, 2024

Accepted Nov 28, 2024

Keywords:

Artificial neural network

Battery storage

Deep learning

Genetic algorithms

Maximum power point tracking

Photovoltaic

Stand-alone system

ABSTRACT

This paper explores optimizing and sizing stand-alone solar power systems using an intelligent maximum power point tracking (MPPT) method, enhanced by artificial neural networks (ANN). The study focuses on both system sizing and energy optimization, integrating genetic algorithms (GA) with deep learning (DL) to optimize the architecture of the ANN for improved performance in predicting solar energy output. The hybrid method, deep learning genetic algorithms (DLGA), efficiently reduces computational complexity and enhances flexibility through parameter tuning, significantly improving the performance of multi-layer perceptron networks. Additionally, a precise sizing methodology based on solar irradiance data was implemented to ensure the system is neither oversized nor undersized. The system's performance was tested and validated using MATLAB/Simulink simulations, which demonstrated superior predictive accuracy, faster convergence, and optimized energy capture. This combined approach of intelligent MPPT and accurate sizing presents a highly effective solution for improving the efficiency and reliability of stand-alone solar energy systems under varying environmental conditions.

This is an open access article under the [CC BY-SA](#) license.



Corresponding Author:

Moufida Saadi

Electrical and Engineering Laboratory (LABGET), Faculty of Electrical Engineering

University of Tebessa

Tebessa 12000, Algeria

Email: saadimoufida8@gmail.com

1. INTRODUCTION

The shift to sustainable energy solutions increasingly highlights stand-alone photovoltaic (PV) systems as promising alternatives to traditional power sources. These systems generate electricity from sunlight, an inexhaustible source that emits no greenhouse gases, making them crucial to renewable energy transitions, especially in remote areas outside conventional grid reach. For self-sufficiency, efficient battery storage and accurate sizing of components, like solar panels and batteries, are vital for continuous, cost-effective power supply [1]–[3].

Sizing optimization determines the best PV configuration to meet energy needs without waste [4]. Various methods are used for this purpose, each with specific advantages and limitations [5]. One common approach, the 'monthly average solar radiation' method, leverages historical solar data to balance energy generation and storage effectively in regions with stable weather [6]. Yet, it may be less accurate in areas with high solar variability [7]. The 'peak sun hours' method simplifies sizing by using peak sunlight hours, but its simplicity can reduce accuracy [8]. More advanced methods, like 'hybrid simulation-optimization,' combine simulation with optimization algorithms to adapt to specific conditions, though they require high computational resources [9], [10]. AI-based approaches, including machine learning and neural networks, are

emerging for PV sizing, yielding accurate predictions when quality data is available [11], [12]. Optimization strategies further enhance PV system performance, including strategic panel placement, effective battery management, and maximum power point tracking (MPPT) for optimal energy conversion under changing environmental conditions [13]–[15]. MPPT significantly boosts energy yields in regions with variable weather, while advanced techniques like artificial neural networks (ANN) and deep learning genetic algorithms (DLGA) refine optimization, improving energy management accuracy and adaptability in diverse environments [16]–[19].

The structure of the paper is methodically organized to facilitate understanding the process of precise sizing and optimization of stand-alone PV systems. Section 2 discusses the modeling and sizing methodologies for these systems. Section 3 reviews recent advancements in intelligent MPPT techniques. Section 4 focuses on the application of ANN and DLGA in optimizing MPPT, while section 5 presents and analyzes the research findings. Finally, section 6 summarizes the study's key insights and conclusions, highlighting the potential for future research and development.

2. MODELING AND SIZING STAND-ALONE SYSTEM

The components of a typical isolated system powered by solar energy, supplemented with battery storage, are modeled mathematically. This system is represented as a stand-alone configuration in Figure 1. To achieve energy self-sufficiency, the final system configuration consists of the following elements:

- A 1.2 kW solar power unit, comprising 16 PV panels, connected to a DC-DC converter and interfaced with the direct current (DC) bus.
- Two batteries, each with a capacity of 100 Ah and a voltage of 12 V, integrated into the system via a bidirectional DC-DC converter. Both batteries share the same connection point and are connected to the DC bus through both alternating current (AC)/DC and DC-DC converters.

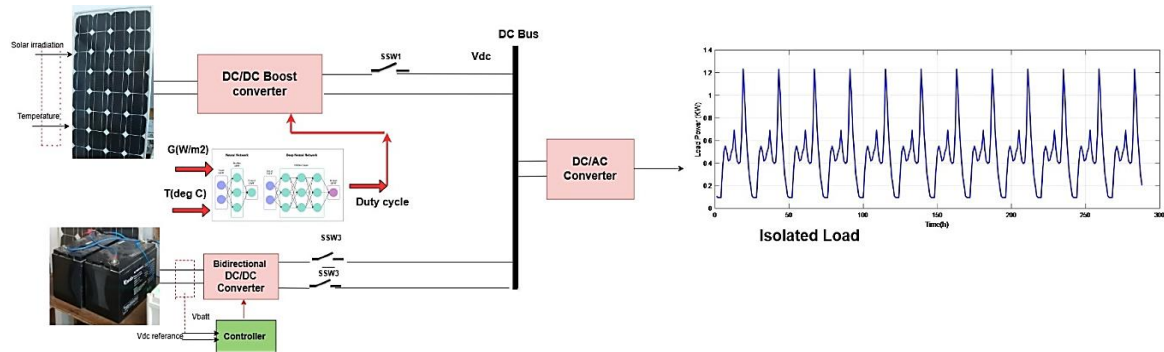


Figure 1. System components and description

In this section, we delve into a detailed exploration of a power system, focusing on the intricacies of modeling its various components. The equilibrium of power within the DC bus can be formulated as (1).

$$P_L(t) = \eta_{DA}(\eta_{DA}P_{PV}(t) \pm \eta_{DD}P_b(t)) \quad (1)$$

In this equation, $P_{PV}(t)$ and $P_b(t)$ represent the power outputs from the PV array and the battery bank, respectively. The constants η_{DD} , η_{DA} denote the efficiencies of the DC/DC and DC/AC power converters. For the purpose of this analysis, these efficiencies are assumed to be constant, with $\eta_{DD} = 0.95$ and $\eta_{DA} = 0.9$. The sign convention for $P_b(t)$ designates it as negative when the battery is charging and positive when discharging. However, it is essential to note that power balance is constrained by certain physical and operational limitations.

$$\begin{aligned} 0 &\leq P_{PV}(t) \leq P_{PV}^{av}(t) \\ P_b^{min} &\leq P_b(t) \leq P_b^{max} \end{aligned} \quad (2)$$

Where P_{PV}^{av} represents the available power generation from the PV array P_b^{min} and P_b^{max} refer to the minimum and maximum battery bank power, respectively [20].

2.1. Photovoltaic array

The power transmission to the generator shaft in a PV system refers to the conversion of incident solar radiation into electrical power. This conversion process is accomplished through the operation of the PV panels [21]. The power transmitted to the generator shaft, represented by (3), is a function of the available solar radiation, n_{pv} the efficiency of the PV panels, A_{pv} surface area of the PV panels, B_{pv} the temperature coefficient for the PV panels. This equation quantifies the power output of the PV system, providing valuable insights into its capacity to generate electrical energy from sunlight.

$$P_{pv}(t) = A_{pv} \cdot G(t) \cdot n_{pv} \cdot (1 + B_{pv} \cdot (T(t) - T_{ref})) \quad (3)$$

Where T_{ref} reference temperature is temperature as a function of time and G is the solar radiation as a function of time. The average power of P_{pv} over the specified time period τ can be calculated using (4).

$$P_{pv}^{av} = \frac{1}{\tau} \int_0^\tau A_{pv} \cdot G(t) \cdot n_{pv} \cdot (1 + \beta_{pv} \cdot (T(t) - T_{ref})) \cdot dt \quad (4)$$

2.2. Storage of energy

Lead-acid batteries used in PV-wind systems function under defined conditions. In the typical operational state, it is difficult to anticipate whether energy will be drawn from or supplied to the battery [22]. Each battery within the energy storage system is depicted as an equivalent circuit, comprising a voltage source (representing open circuit voltage, V_{oc}) in series with an internal resistance (R_{int}) [23]. As a result, the terminal voltage of the battery is established by (5).

$$V_{batt} = V_{oc} - R_{int} I_{bat} \quad (5)$$

In this model, both V_{oc} and R_{int} are dependent on the battery's state of charge (SOC_b), which indicates the remaining capacity available for discharge. This correlation is represented as data vectors, with their values determined through interpolation within the respective vector based on the current SOC_b . This accommodates the nonlinear interdependencies between V_{oc} and R_{int} . The state of charge SOC_b can be expressed as (6).

$$SOC_b = \frac{C_b^{*,max} - C_b^{*,u}}{C_b^{*,max}} 100 \quad [\%] \quad (6)$$

Where $C_b^{*,u}$ represents the number of ampere-hours already utilized and $C_b^{*,max}$ signifies the maximum capacity, measured in ampere-hours. This can be computed as (7).

$$C_b^{*,u} = \int_0^t \frac{I_b \eta_c}{3600} dt \quad [Ah] \quad (7)$$

Where η_c denotes the charge/discharge battery Coulombic efficiency, which is 0.975 in this case. I_b signifies the battery current in amperes, with $I_b > 0$ indicating discharge and $I_b < 0$ indicating charging. The initial SOC_b is determined by a nonzero initial value of $C_b^{*,u}$. To ensure optimal performance and battery longevity, SOC_b must be maintained within specific limits, defined as $SOC_{bmin} \leq SOC_b \leq SOC_{bmax}$.

The battery current is subject to constraints, and these limits are contingent on V_{oc} and R_{int} , as described by (8).

$$I_b^{lim} = \begin{cases} \frac{(V_{oc} - V_b^{max})}{R_{int}} & \text{during of charge} \\ \frac{(V_{oc} - V_b^{min})}{R_{int}} & \text{during of discharge} \end{cases} \quad (8)$$

V_b^{min} and V_b^{max} represent the minimum and maximum permissible battery bank voltages, respectively. Furthermore, I_b^{lim} is indirectly influenced by SOC_b through the previously mentioned nonlinear relationships. Additionally, a mechanism is in place to limit the battery bank current, ensuring zero current when SOC_b reaches its maximum or minimum value [24].

3. SIZING STAND-ALONE SYSTEM BASED ON MONTHLY AVERAGE METHOD

The effective and dependable functioning of a stand-alone photovoltaic/battery system relies heavily on accurate sizing. Sizing this system utilizing monthly average data entails establishing the suitable capacities for the PV panels and energy storage elements, which are crucial in proficiently fulfilling the load demands (refer to Table 1). The general load, PV, and energy produced are given by (9) and (10).

$$E_{load} = E_{PV} S_{PV} \quad (9)$$

$$E_{PV} = S_{PV} E_{irr} \eta_{PV} \quad (10)$$

With:

$$\eta_{PV} = \eta_{PV-STC} [1 - \beta_{oc}(T_j - T_{j-STC})] \quad (11)$$

Through rigorous computations of monthly energy yield for each generator and corresponding load demand, distinct surface areas for photovoltaic panels are discerned. These quantifications are deduced using the formulations presented for PV, as elucidated in [25].

$$S_{PV} = \max \left(\frac{E_{Load,m}}{E_{PV,m}} \right) \quad (12)$$

The Montney energies produced by PV are given in (13).

$$\begin{cases} E_{PV,m} = (\sum_{m=1}^{12} E_{PV})/12 \\ E_{Load,m} = (\sum_{m=1}^{12} E_{Load})/12 \end{cases} \quad (13)$$

Here, Elmean represents the energy required to meet the load demand. It is calculated as the average energy needed to satisfy the system's load demand under various configurations of wind turbines and photovoltaic panels. K_{perc} represents the proportion of the load supplied by the PV source. Consequently, we derive the following result, as expressed in (14).

$$S_{PV} = K_{perc} \left(\frac{E_{Load,aver}}{E_{PV,ave}} \right) \quad (14)$$

The subsequent equations establish the quantities of PV panels required, as expressed in (15).

$$S_{PV,final} = N_{PV} S_{PV,unit} \quad (15)$$

The mean energy consumption is expressed as (16).

$$E_{load-ave} = E_{PV,ave} S_{PV,unit} \quad (16)$$

Table 1. The setup and parameters of the PV and wind energy systems

Month	E_{irr} (KWh/m)	T (°C)	N_{PV}	E_{PV} (KWh/m ²)	E_{load} (KWh)
January	85.5	10.1	0.1410	7.78	333.6
February	98.6	11.5	0.1419	9.03	339
March	143.6	16.1	0.1446	13.41	347
April	174.2	19.8	0.1468	16.51	347.04
May	201.5	24.5	0.1497	19.48	336.72
June	207.3	28.7	0.1486	19.89	332.88
July	218.2	32.3	0.1539	21.74	347.04
August	197.1	31.6	0.1512	19.59	345.84
September	156.4	27.1	0.1512	15.27	336.48
October	127.9	22.7	0.1485	12.26	323.52
November	95	15.5	0.1443	8.85	343.44
December	79.6	11.1	0.1416	7.28	329.52
$E_{PV, ave} = 13.42$					
$E_{load, ave} = 338.5$					

The sizing parameters for the hybrid system are determined based on the previously outlined relationships. Table 2 provides a breakdown of the monthly energy production from the solar system. It can be noted that the average photovoltaic energy output is approximately 13.42 kWh/m². Given that the average load energy demand is 338.5 kWh, and considering that the system in question is a stand-alone PV system, only the configuration of 40 panels comes closest to meeting the required load energy of 523.47 kWh.

Battery capacity is calculated using the annual monthly average method with the day of autonomy, as expressed in (17).

$$C_{batt} = \frac{d_{aut} \cdot E_{load,m}}{U_{batt} \cdot PDP \cdot \eta_{batt} \cdot N_m} \quad (17)$$

Where $E_{load,m}$ monthly load consumed (kWh/d) and N_m the number of days of the month that presents the maximum load (31 days), PDP stands for percentage depth of discharge η_{batt} . The efficiency of the battery. The number of batteries used is calculated by (18).

$$N_{batt} = ENT\left[\frac{C_{batt}}{C_{batt-u}}\right] \quad (18)$$

Where C_{batt-u} represents the selected battery capacity. To summarize, the total maximum power output of the photovoltaic panels is determined as $P_{pv} = 40 \times 80 = 3,600$ kW. Moreover, the system utilizes 3 batteries with specifications of (12 V, 100 Ah).

Table 2. The number of wind turbines and panels was determined through

K_{perc}	S_{PV} (m ²)	N_{PV}	S_{PV} , final (m ²)	Elmean (Kwh)
0	0	0	0	0
0.1	4.28	7	4.522	60.68
0.2	7.5	12	7.752	104.03
0.3	7.76	12	7.752	104.03
0.4	8.40	13	8.39	112.59
0.5	8.64	13	8.398	112.70
0.6	10.04	16	10.336	198.70
0.7	11.17	17	10.98	147.35
0.8	14.12	23	14.858	199.28
0.9	19.83	31	20.02	268.66
1	26.38	40	26.48	345.36

4. APPLICATION OF HYBRID INTELLIGENT MPPT (DLGA)

The application of ANN in maximum power point (MPP) Tracking is particularly essential due to solar energy's inherently variable nature, which is affected by a range of environmental conditions, including the intensity of sunlight, temperature, and shadow impacts. ANN functions similarly to the human brain by learning and retaining information and insights through a network of interconnected links known as weights. For precise identification of the MPP, these weights associated with the neurons must be meticulously calculated via an extensive training process. Once this training is complete, the ANN can serve as an estimator for the MPP, providing the reference value (maximum power voltage (VMP) or maximum power current (IMP)) to the MPPT controller [26].

The training of an ANN involves a systematic adjustment of weights and biases, often utilizing the sigmoid activation function. Initially, weights and biases are randomly assigned to set the starting point for the learning process. During forward propagation, inputs pass through the network, with each neuron calculating a weighted sum and adding a bias, subsequently passed through an activation function like a sigmoid. The sigmoid function, mapping values between 0 and 1, is favored for its ability to convert numbers into probabilities and handle non-linear data relationships. Following this, the backpropagation phase begins, where the network's output error is calculated and propagated backward, adjusting weights and biases. This adjustment is based on the error's partial derivatives concerning each weight and bias, guided by a learning rate parameter. This cycle of forward propagation, backpropagation, and weight and bias adjustments repeats over multiple iterations, gradually refining the network to minimize prediction errors. The training process also includes evaluating and adjusting the model with a validation set to prevent overfitting or underfitting, ensuring the ANN effectively generalizes to new data. In ANNs, an increase in the number of hidden layers can lead to enhanced tracking efficiency and improved performance in adapting to power fluctuations in the array, though it may also result in slower tracking speed.

The integration GA with DL for the optimization of ANN architectures has been a focus of various researchers. This approach aims to enhance the performance of multi-layer perceptron networks. Given the computational complexity and extended training duration inherent in DL evolutionary algorithms like GA are employed to optimize network performance. GA is particularly noted for its robust optimization capabilities. This method effectively reduces computational complexity and increases overall system flexibility through parameter tuning, thereby augmenting the performance of DL. In this scheme, DL is utilized to determine the optimal duty cycle value, ensuring maximum power extraction. The neural network undergoes training with a dataset, which is then optimized using GA for improved efficiency. The steps involved in implementing the genetic algorithm are outlined as follows:

- Step I: Assess the fitness function and pinpoint the design parameters.
- Step II: Generate a population, representing potential solutions to the problem.
- Step III: Evaluate this population using an objective function.
- Step IV: From the population, select two parents based on their fitness levels. Higher fitness increases the likelihood of selection.
- Step V: Create a new population by repeatedly executing selection, crossover, and mutation until the new population is complete.
- Step VI: Form a new generation and return to step III.
- Step VII: If the end condition (minimization of mean squared error (MSE)) is met, conclude the process and identify the best solution as the target (see Figure 2).

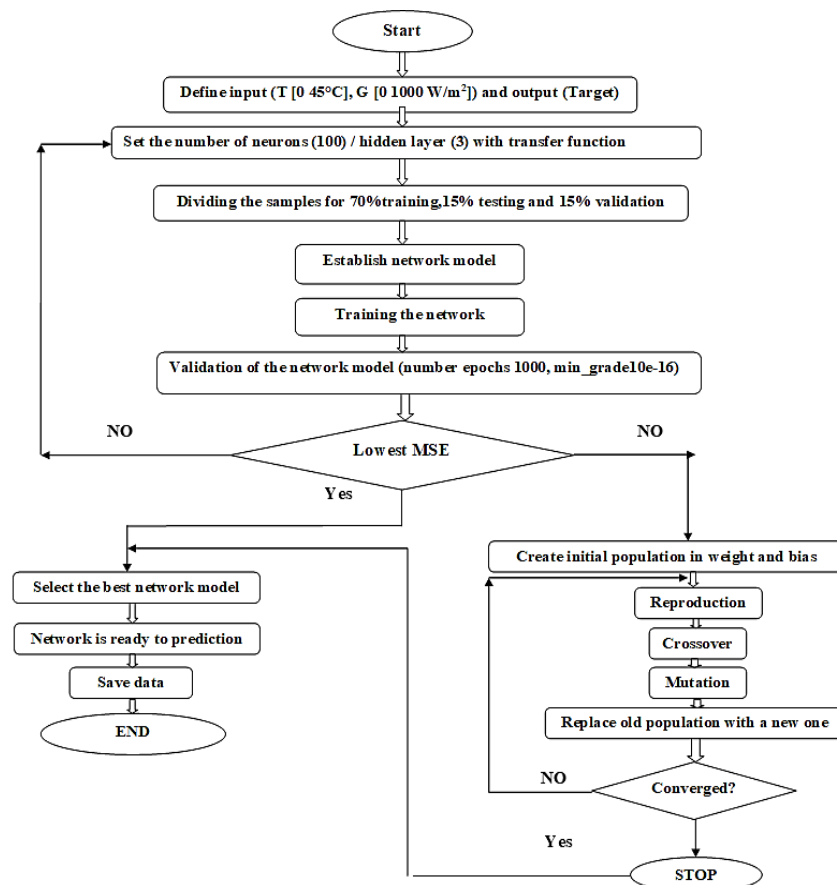


Figure 2. Block diagram training MPPT using DLGA

Figure 3 illustrates the training dynamics of different ANN architectures: ANN with 10 neurons, ANN with 100 neurons, deep learning (DL), and DLGA, represented as Figures 3(a)-3(d), respectively. Among these, DLGA (Figure 3(d)) shows the best performance, with rapid convergence and low mean squared error (MSE) across training, validation, and test phases, indicating a highly generalizable model. Figure 3(a) shows initial improvement but reaches a plateau, while Figure 3(b) exhibits overfitting, as seen in the rise of validation error after initial progress. Figure 3(c), like Figure 3(a), fits the data decently but shows

a slight divergence between training and validation errors, suggesting possible overfitting. Overall, DLGA proves to be the most robust, making it the optimal choice for real-world applications due to its superior accuracy and generalization. Table 3 provides a detailed comparison of the architectures based on key metrics like epoch range (0 to 1000), training time, overall performance, and gradient behavior. These metrics offer insights into the efficiency and effectiveness of each model, with the gradient target set at $1\text{e-}16$, reflecting a high precision in the learning process.

Table 3. Comparison between performances of different architecture of ANN

ANN architecture	Number of epochs	Elapsed time (s)	Performance	Gradient
ANN 10N	1000	00 :00 :04	$1.44\text{ e-}14$	$9.45\text{ e-}14$
ANN 100 N	1000	00 :00 :08	$1.33\text{ e-}14$	$7.32\text{ e-}11$
DL	1000	00 :00 :15	$4.09\text{ e-}12$	$9.68\text{ e-}9$
DL GA	14	00:14:37	$3.47\text{e-}32$	$5.16\text{ e-}17$

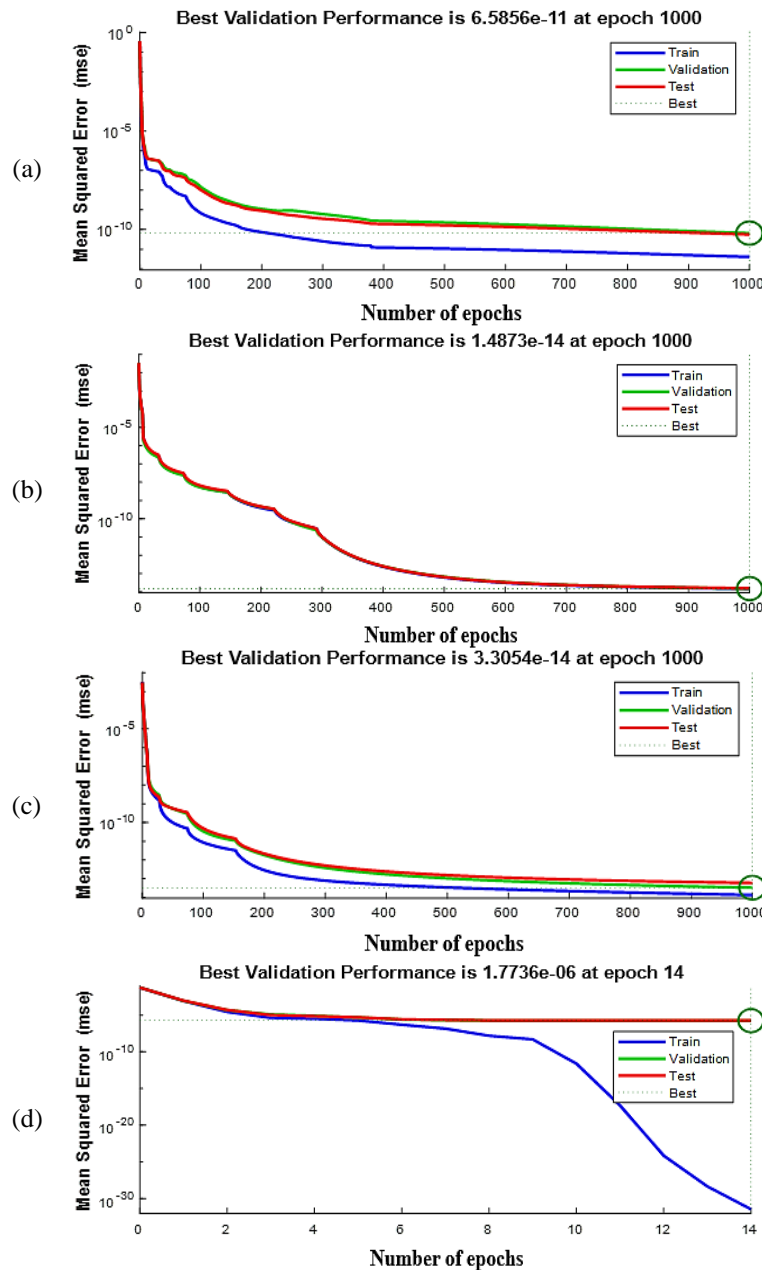


Figure 3. The dynamic training of various ANN architectures: (a) ANN with 10 neurons, (b) ANN with 100 neurons, (c) deep learning (DL), and (d) DLGA

5. DISCUSSION OF RESULTS

Set within the specific environmental conditions of Negrine, Wilaya of Tebessa in Algeria, the study utilizes historical atmospheric data from 2012, including variables like ambient temperature and solar insolation, to accurately size and optimize the system as shown in Figure 4. The system, comprising PV panels and battery storage, was simulated in MATLAB/Simulink using localized data and load profiles, showcasing the effectiveness of ANN-optimized MPPT in improving power generation to meet varying energy demands. The study provides valuable insights into the deployment of efficient solar energy systems in arid and semi-arid regions.

Figure 5 presents the power generated by the PV and wind turbine is depicted alongside the load profile. This figure helps visualize how the combined energy production from these renewable sources aligns with the demand requirements. By comparing these curves, one can assess whether the generated power meets, exceeds, or falls short of the load at various points in time.

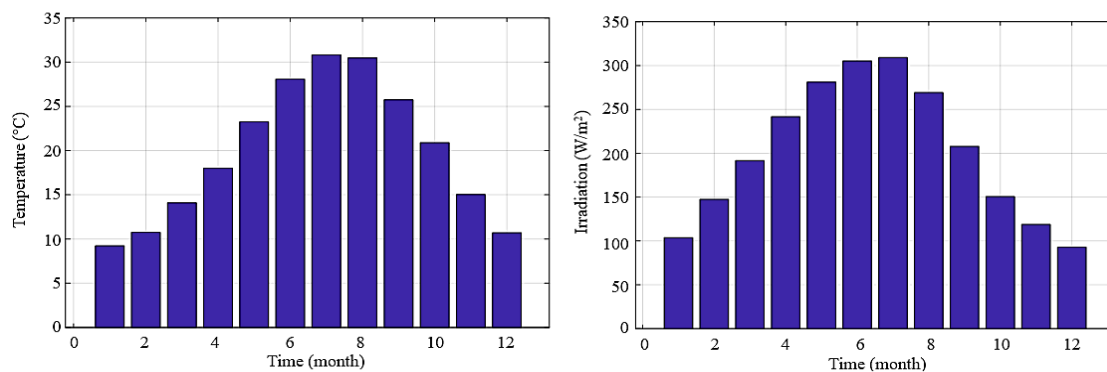


Figure 4. Historical data ambient temperature and solar insolation in one year

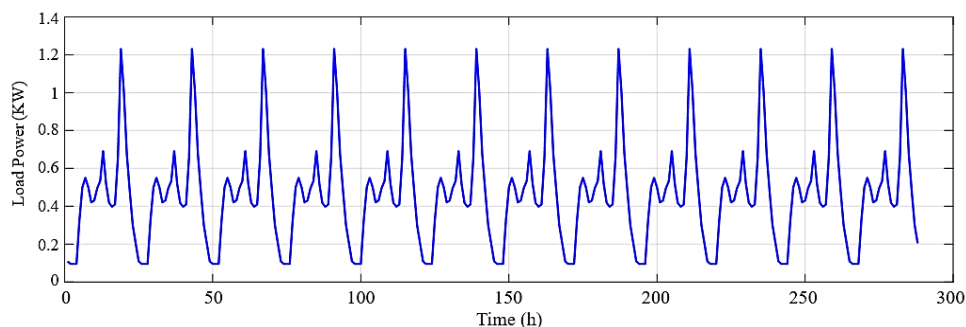


Figure 5. Power load profile chosen

Figure 6 presents a comparative analysis of two MPPT methods: DLGA and perturb and observe (P&O), applied to a stand-alone PV system, focusing on DC bus voltage. Over 12 hours, the DLGA consistently maintains a higher and more stable voltage than P&O. While P&O shows a step-like increase during its initial ramp-up, indicating its iterative approach, DLGA demonstrates a smoother and quicker convergence to the maximum power point. This is likely due to DLGA's predictive capabilities, which use historical data for more precise control. The zoomed-in view reveals that DLGA has minimal ripple and tighter voltage regulation, suggesting better handling of variable environmental conditions, while P&O shows more pronounced voltage fluctuations, indicating less stability. DLGA's stability reduces power oscillations, enhancing system efficiency and minimizing wear on components.

Figure 7 compares the performance of four MPPT techniques: DLGA, DL, ANN, and P&O, over 12 hours in a PV system. DLGA, ANN, and DL demonstrate a swift and stable rise to peak power, with DLGA showing superior stability and minimal fluctuations. As solar irradiance changes, DLGA adapts well, maintaining near-optimal power around 880 W, while P&O experiences a larger dip to 780 W. During peak midday irradiance, DLGA sustains around 1550 W, outperforming P&O, which fluctuates near 1500 W. ANN and DL match DLGA at 1350 W but show a less dynamic response to irradiance changes. As sunlight wanes, DLGA maintains the highest output (850 W), while P&O declines more erratically, and ANN/DL drop more sharply.

Figure 8, depicting battery power output, shows that DLGA stabilizes quickly, maintaining consistent power with minimal fluctuation, indicating efficient battery management. In contrast, P&O exhibits more pronounced fluctuations, suggesting less efficient battery charge regulation. As the system transitions to discharging, DLGA handles the shift smoothly, while ANN and DL mirror each other closely in performance. Overall, DLGA stands out for its robustness and adaptability, ensuring maximum battery efficiency and system energy availability throughout the day.

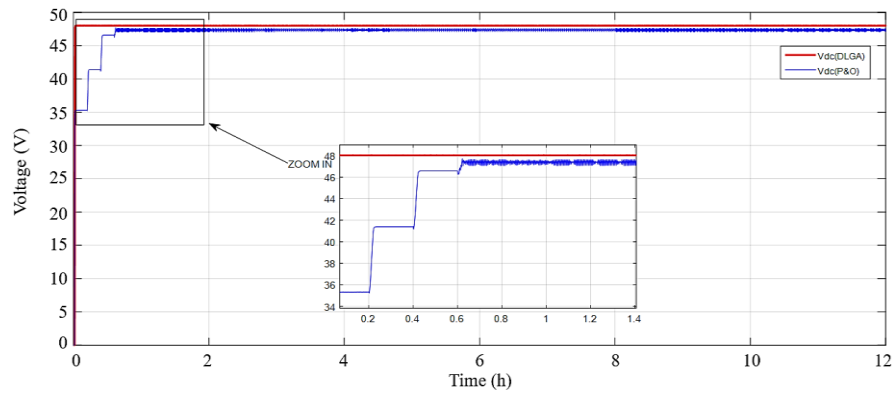


Figure 6. Profile of voltage DC bus in 12 hours

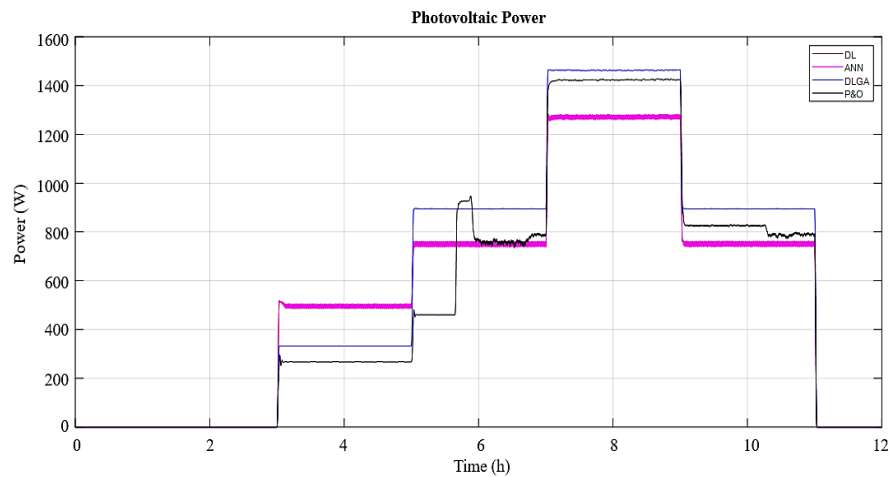


Figure 7. Profile of a PV power in the 12 hours

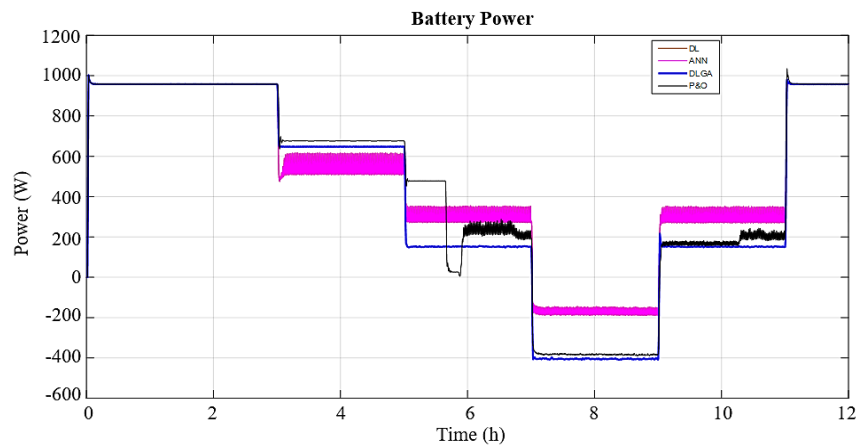


Figure 8. Profile of a battery power in the 12 hours

6. CONCLUSION

This study investigated the optimization of a stand-alone solar power system by improving MPPT algorithms using ANN and genetic algorithms (GA), specifically the DLGA approach. The results, based on simulations using atmospheric data from Negrine, Algeria, showed that the DLGA method outperforms traditional techniques like P&O in maintaining higher, more stable voltages, leading to improved energy capture. The DLGA also demonstrated superior performance in managing battery charging and discharging cycles, enhancing battery efficiency and lifespan. Additionally, the ANN models showed effective power management, and mean squared error analysis confirmed excellent generalization capabilities in the ANN training process. Overall, this research highlights the potential of intelligent MPPT methods to optimize solar energy systems, offering more reliable and efficient solutions for regions with high solar potential. The methodologies presented can serve as a benchmark for future renewable energy optimization efforts.

FUNDING INFORMATION

No funding involved.

AUTHOR CONTRIBUTIONS STATEMENT

This journal uses the Contributor Roles Taxonomy (CRediT) to recognize individual author contributions, reduce authorship disputes, and facilitate collaboration.

Name of Author	C	M	So	Va	Fo	I	R	D	O	E	Vi	Su	P	Fu
Moufida Saadi	✓	✓	✓	✓	✓	✓		✓	✓	✓			✓	✓
Dib Djalel		✓				✓		✓	✓	✓	✓	✓		✓
Kadir Erkan	✓		✓	✓			✓			✓	✓		✓	

C : Conceptualization

M : Methodology

So : Software

Va : Validation

Fo : Formal analysis

I : Investigation

R : Resources

D : Data Curation

O : Writing - Original Draft

E : Writing - Review & Editing

Vi : Visualization

Su : Supervision

P : Project administration

Fu : Funding acquisition

CONFLICT OF INTEREST STATEMENT

Authors state no conflict of interest.

DATA AVAILABILITY

Data availability is not applicable to this paper as no new data were created or analyzed in this study.




REFERENCES

- [1] S. Ahmad *et al.*, "A Review of Hybrid Renewable and Sustainable Power Supply System: Unit Sizing, Optimization, Control, and Management," *Energies* (19961073), vol. 17, no. 23, p. 6027, 2024, doi: 10.3390/en17236027.
- [2] O. Hafez and K. Bhattacharya, "Optimal planning and design of a renewable energy based supply system for microgrids," *Renewable Energy*, vol. 45, pp. 7–15, Sep. 2012, doi: 10.1016/j.renene.2012.01.087.
- [3] H. Rezzouk and A. Mellit, "Feasibility study and sensitivity analysis of a stand-alone photovoltaic–diesel–battery hybrid energy system in the north of Algeria," *Renewable and Sustainable Energy Reviews*, vol. 43, pp. 1134–1150, Mar. 2015, doi: 10.1016/j.rser.2014.11.103.
- [4] G. Zubi, R. Dufo-López, M. Carvalho, and G. Pasaoglu, "The lithium-ion battery: State of the art and future perspectives," *Renewable and Sustainable Energy Reviews*, vol. 89, pp. 292–308, Jun. 2018, doi: 10.1016/j.rser.2018.03.002.
- [5] R. Luna-Rubio, M. Trejo-Perea, D. Vargas-Vázquez, and G. J. Ríos-Moreno, "Optimal sizing of renewable hybrids energy systems: a review of methodologies," *Solar Energy*, vol. 86, no. 4, pp. 1077–1088, Apr. 2012, doi: 10.1016/j.solener.2011.10.016.
- [6] G. Merei, C. Berger, and D. U. Sauer, "Optimization of an off-grid hybrid PV–wind–diesel system with different battery technologies using genetic algorithm," *Solar Energy*, vol. 97, pp. 460–473, Nov. 2013, doi: 10.1016/j.solener.2013.08.016.
- [7] R. Sen and S. C. Bhattacharyya, "Off-grid electricity generation with renewable energy technologies in India: an application of HOMER," *Renewable Energy*, vol. 62, pp. 388–398, Feb. 2014, doi: 10.1016/j.renene.2013.07.028.
- [8] A. Mellit and S. A. Kalogirou, "Artificial intelligence techniques for photovoltaic applications: a review," *Progress in Energy and Combustion Science*, vol. 34, no. 5, pp. 574–632, Oct. 2008, doi: 10.1016/j.pecs.2008.01.001.
- [9] H. X. Yang, L. Lu, and J. Burnett, "Weather data and probability analysis of hybrid photovoltaic–wind power generation systems in Hong Kong," *Renewable Energy*, vol. 28, no. 11, pp. 1813–1824, Sep. 2003, doi: 10.1016/S0960-1481(03)00015-6.
- [10] A. A. Abou El Ela, M. A. Abido, and S. R. Spea, "Optimal power flow using differential evolution algorithm," *Electric Power Systems Research*, vol. 80, no. 7, pp. 878–885, Jul. 2010, doi: 10.1016/j.epsr.2009.12.018.
- [11] D. Yue, F. You, and S. B. Darling, "Domestic and overseas manufacturing scenarios of silicon-based photovoltaics: Life cycle energy and environmental comparative analysis," *Solar Energy*, vol. 105, pp. 669–678, 2014, doi: 10.1016/j.solener.2014.04.008.




- [12] S. Sinha and S. S. Chandel, "Review of recent trends in optimization techniques for solar photovoltaic–wind based hybrid energy systems," *Renewable and Sustainable Energy Reviews*, vol. 50, pp. 755–769, Oct. 2015, doi: 10.1016/j.rser.2015.05.040.
- [13] P. Paliwal, N. P. Patidar, and R. K. Nema, "Determination of reliability constrained optimal resource mix for an autonomous hybrid power system using particle swarm optimization," *Renewable Energy*, vol. 63, pp. 194–204, Mar. 2014, doi: 10.1016/j.renene.2013.09.003.
- [14] H. Patel and V. Agarwal, "Maximum power point tracking scheme for PV systems operating under partially shaded conditions," *IEEE Transactions on Industrial Electronics*, vol. 55, no. 4, pp. 1689–1698, Apr. 2008, doi: 10.1109/TIE.2008.917118.
- [15] K. Karabacak and N. Cettin, "Artificial neural networks for controlling wind–PV power systems: A review," *Renewable and Sustainable Energy Reviews*, vol. 29, pp. 804–827, Jan. 2014, doi: 10.1016/j.rser.2013.08.070.
- [16] A. Y. Taha, M. Aljanabi, A. N. Al-Shamani, and Z. H. Hadi, "Intelligent maximum power point tracking for photovoltaic system using meta-heuristic optimization algorithms: A holistic review," *AIP Conference Proceedings*, 2023, vol. 2776, no. 1, p. 050003, doi: 10.1063/5.0136227.
- [17] E. Koutroulis, D. Kolokotsa, A. Potirakis, and K. Kalaitzakis, "Methodology for optimal sizing of stand-alone photovoltaic/wind-generator systems using genetic algorithms," *Solar Energy*, vol. 80, no. 9, pp. 1072–1088, 2006, doi: 10.1016/j.solener.2005.11.002.
- [18] M. L. T. Zulu, R. P. Carpanen, and R. Tiako, "A Comprehensive Review: Study of Artificial Intelligence Optimization Technique Applications in a Hybrid Microgrid at Times of Fault Outbreaks," *Energies*, vol. 16, no. 4, p. 1786, 2023, doi: 10.3390/en16041786.
- [19] A. G. Abo-Khalil and D. -C. Lee, "MPPT control of wind generation systems based on estimated wind speed using SVR," *IEEE Transactions on Industrial Electronics*, vol. 55, no. 3, pp. 1489–1490, Mar. 2008, doi: 10.1109/TIE.2007.907672.
- [20] D. Feroldi and D. Zumoffen, "Sizing methodology for hybrid systems based on multiple renewable power sources integrated to the energy management strategy," *International Journal of Hydrogen Energy*, vol. 39, no. 16, pp. 8609–8620, May 2014, doi: 10.1016/j.ijhydene.2014.01.003.
- [21] A. Z. Sahin, K. G. Ismaila, B. S. Yilbas, and A. Al-Sharafi, "A review on the performance of photovoltaic/thermoelectric hybrid generators," *International Journal of Energy Research*, vol. 44, no. 5, pp. 3365–3394, Apr. 2020, doi: 10.1002/er.5139.
- [22] A. A. Kebede *et al.*, "Techno-economic analysis of lithium-ion and lead-acid batteries in stationary energy storage application," *Journal of Energy Storage*, vol. 40, p. 102748, Aug. 2021, doi: 10.1016/j.est.2021.102748.
- [23] D. P. Jenkins, J. Fletcher, and D. Kane, "Lifetime prediction and sizing of lead–acid batteries for microgeneration storage applications," *IET Renewable Power Generation*, vol. 2, no. 3, pp. 191–200, 2008, doi: 10.1049/iet-rpg:20080021.
- [24] V. H. Johnson, "Battery performance models in ADVISOR," *Journal of Power Sources*, vol. 110, no. 2, pp. 321–329, Aug. 2002, doi: 10.1016/S0378-7753(02)00194-5.
- [25] D. Rekioua, T. Rekioua, A. Elsanabary, and S. Mekhilef, "Power management control of an autonomous photovoltaic/wind turbine/battery system," *Energies*, vol. 16, no. 5, p. 2286, Feb. 2023, doi: 10.3390/en16052286.
- [26] M. N. Ali, K. Mahmoud, M. Lehtonen, and M. M. F. Darwish, "Promising MPPT methods combining metaheuristic, fuzzy-logic and ANN techniques for grid-connected photovoltaic," *Sensors*, vol. 21, no. 4, p. 1244, Feb. 2021, doi: 10.3390/s21041244.

BIOGRAPHIES OF AUTHORS






Moufida Saadi    is a Ph.D. student at the University of Tebessa in Algeria. She specializes in renewable energy and the application of artificial intelligence. Her work primarily involves integrating AI technologies with renewable energy systems to enhance efficiency and sustainability. Her research is focused on developing intelligent algorithms for managing solar and wind energy, contributing significantly to the advancement of green technology. She has made her mark by presenting my findings at various international conferences and publishing papers in emerging energy journals. Her academic journey includes a master's degree in electrical engineering with a specialization in renewable energy. She can be contacted at email: Moufida.saadi@univ-tebessa.dz.



Dib Djalel    is a full professor and currently works as a research director in the Department of Electrical Engineering at the University of Tebessa in Algeria. He received his Ph.D. in power systems in 2007 in Algeria, and he was awarded the professor rank in December 2015. He holds the position of research director and head of the electrical engineering team at LABGET and LM laboratory at the University of Tebessa. He participated in several conferences and published several papers, now he is a reviewer for several journals. His research interests are power grids, power quality, and renewable energy. He can be contacted at email: dibdjalel@gmail.com.



Kadir Erkan    is an associate professor at Yildiz Technical University in the Department of Mechatronics Engineering. He received his Ph.D. in electrical engineering and specializes in the design and control of electromagnetic systems, micro-robotics, and magnetic levitation. Erkan has participated in numerous international conferences and has published extensively on topics such as hybrid electromagnetic systems and precise control techniques in mechatronics. His research contributions have been instrumental in advancing the fields of robotics, automation, and control systems. He can be contacted at email: kadirerkan03@gmail.com.